Journal of KSNVE, Vol. 7, No. 2, pp. 231~238, 1997.

(Original Paper)

Development of An Automated Scanning Laser Doppler Vibrometer For Measurements of In-Plane Structural Vibration

평면 구조 진동 측정을 위한 자동화된 스캐닝 레이저 도플러 진동측정기의 개발 및 연구

Hyun-Gwon Kil

길 현 권*

(Received November 8, 1996; Accepted December 19, 1996)

Key Words : Automated Scanning Laser Doppler Vibrometer, In-Plane Vibration Measurement

ABSTRACT

An automated scanning laser Doppler vibrometer (LDV) has been designed, and built to measure in-plane vibration fields over structures. Use of optical fibers allows the compact design of a laser probe head which can be scanned over the vibrating structures. An algorithm for automated self -alignment of the laser probe is developed. The system is completely automated for scanning over the structures, focusing two laser beams at each data point until the detected vibration signal is stable, and for recording and transferring the data to a system computer. The automated system allows one to get extensive data of the vibration field over the structures. The system is tested by scanning a piezoelectric cylindrical shell and a plate excited by a continuous signal and by a pulse signal, respectively. Results show that the automated scanning LDV system can be a useful tool to measure the in-plane vibration field and to detect the elastic waves propagating on the vibrating structures.

요 약

진동하는 구조물의 평면 진동장을 측정하기 위해, 자동화된 스캐닝 레이저 도플러 진동 측정기를 개발하고 이의 성능을 시험하였다. 광섬유를 사용하여 레이저 탐침이 진동체 표면을 따라 움직일 수 있도록 하였으며, 시스템의 자동화를 이루기 위한 알고리즘을 고안하였다. 시스템의 자동화 과정은, 레이저 탐침이 진동체 표면을 따라 움직이도록 하며, 표면의 각 측정 점마다 두 레이저 광선들의 초점을 맞추고, 진동 신호 데이터를 얻고 저장하는 모든 과정을 포함한다. 따라서 이 자동화 과정을 이용하여 구조물의 표면 진동장을 측정할 수 있도록 하였다. 이 진동 측정기의 성능을 시험하기 위하여, 연속 신호로 가진되는 압전 원통 셸의 진동과 펄스 신호에 의해 가진되는 평판의 진동을 측정하였다. 측정 결과로부터, 구조물의 평면 진동장을 측정하고 표면을 따라 전파되는 탄성파들을 분리해내기 위하여, 이 자동화된 스캐닝 레이저 도플러 진동 측정기가 유용한 측정 도구가 될 수 있음을 보였다.

1. Introduction

There is a need for experimental techniques capable of imaging the state of vibration of shells with internal components such as stiffeners and added masses. Those are required to separate contributions to the structural vibration by in-plane waves (longitudinal and shear waves) and by out-of-plane waves (flexural waves). It is reasoned as follows.

*Member, Department of Mechanical Engineering, Suwon University

When a propagating wave meets the structural discontinuities, the other types of waves can be reflected from or transmitted through them[1]. The wave -propagation phenomenon over the corresponding structures determines the characteristics of the structural vibration, furthermore, the characteristics of sound radiation from the structures. In addition, contributions of in-plane waves and out-of-plane waves to structural energy flow could be equally important[2]. Those reasons lead to a need for measurements of both in-plane and out-of-plane vibrations of the structures.

The laser Doppler vibrometry technique offers the possibility of direct and non-intrusive measurements of both in-plane and out-of-plane vibrations. Most of previous work with the LDV technique in literature has been performed to measure the out-of -plane structural vibration. Monchalin[3] used the LDV technique to measure both in-plane and out-of -plane surface vibrations. Vignola and Houston[4] developed a laser probe to measure the vector displacement (simultaneous measurement of in-plane and out-of-plane components) at a given point on vibrating structures. To measure spatially distributed vibration fields on structures, scanning laser Doppler systems with oscillating mirrors were developed by Sriram, et al[5]. and Dominguez, et al[6]. A mechanically scanned laser probe was developed by Lee, et al[7]. to measure the in-plane vibration of structures. It was successfully used to detect elastic waves on a vibrating cylindrical shell driven with a single frequency signal. However, the measurements are very sensitive to alignment of the laser probe. The probe should be realigned at each data point on the vibrating structure. In addition, in order to identify the elastic waves propagating on the structures, measurements of the vibration field over the structure are required. It is therefore expedient to automate the alignment of the probe, and furthermore, to achieve a completely automated scanning LDV system. It leads to the objective of this work that is to develop an automated scanning laser Doppler vibrometer.

2. Operational Principle of the LDV System

2.1 Optical Phase Change Due to the Surface Vibration

Light waves scattered from the vibrating surface experience an optical phase change due to the instantaneous surface vibration with displacement

$$\boldsymbol{r}=u\boldsymbol{e}_x+w\boldsymbol{e}_z \tag{1}$$

where u and w correspond to in-plane and out-of -plane components of displacement vector $\boldsymbol{r}$, respectively. The phase change due to the in-plane vibration can be detected with the configuration shown in Fig. 1. Two laser beams are projected into a single spot on the surface with an angle 2α between the corresponding incident wave number vectors $\boldsymbol{k}_1$ and $\boldsymbol{k}_2$ which are symmetric with respect to the normal to the surface. The interference of the two speckle fields originating from the incident waves is detected along the direction of $\boldsymbol{k}_0$. In this case, the relative phase change $\Delta\phi$ between beam 1 and 2 is given by[3]

$$\Delta\phi=(\boldsymbol{k}_2-\boldsymbol{k}_1)\cdot\boldsymbol{r}=\frac{4\pi}{\lambda}u\sin\alpha \tag{2}$$

in terms of the in-plane displacement component u. Here, λ is the wavelength of the laser light in vacuum.

2.2 Detection of the Surface Vibration

The interference of scattered light generates the electric current at the photodetector as follows. The total current is proportional to the time average

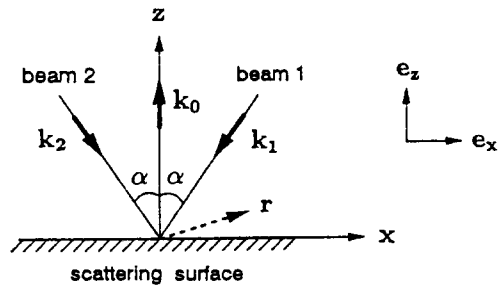

Fig. 1 Optical Configuration for detection of the in -plane surface vibration with a displacement vector $\boldsymbol{r}=u\boldsymbol{e}_x+w\boldsymbol{e}_z$

(over a period equal to the response time of the photodetector) of the square of the total electric fields. The AC current contains the optical phase change due to the surface vibration, and takes the form[8]

$$i_{ac}=CE_1E_2\cos(\omega_B t+\Delta\phi+\Delta\theta) \tag{3}$$

where C is a constant which includes the quantum efficiency and the gain of the photode-tector. E_1 and E_2 are magnitudes of the electric fields of the two scattered light signals. The frequency $w_B=2\pi f_B$ is an additional frequency shift ($f_B=40MHz$), which is required for heterodyne detection[8] of the surface vibration. $\Delta\theta$ is the phase difference of the two light beams incident into the photodetector due to random fluctuations in environmental conditions including temperature fluctuations and random vibrations in the optical system. Considering harmonic surface vibration at frequency w_s with in -plane displacement component $u=A\cos\{w_s t+\psi\}$, the ac current takes the form

$$i_{ac}=CE_1E_2\cos\{w_s t+m(t)+\Delta\theta\} \tag{4}$$

where $m(t)$ is the frequency modulation from the vibrating surface, which takes

$$m(t)=\frac{4\pi A}{\lambda}\sin\alpha\cos(w_s t+\psi) \tag{5}$$

for configurations in Fig. 1.

There are two basic methods to extract information about the modulation index : spectral analysis[9] and FM demodulation[10]. The former has the advantage of being an absolute measurement of the corresponding displacement component. The latter is more appropriate for measurements of transient vibration signals and for detection of elastic waves which require detection of the phases as well as the amplitudes of vibration signals. In the present study the FM demodulation with a phase locked loop (PLL)[10] was implemented. It is breifly described as follows. The carrier frequency (40 MHz) of the photodetector FM signal in Eq. (4) is down-shifted with appropriate mixing to a lower frequency (e. g. 100 kHz). The FM signal of a carrier frequency 100 kHz is given as an input to the PLL. The output signal from the PLL is proportional to the instantaneous deviation of the signal frequency from the carrier frquency, which is given by

$$i_P(t)=K\frac{d}{dt}m(t)$$
$$=-K\frac{4\pi A}{\lambda}w_s\sin\alpha\sin(\omega_s t+\psi) \tag{6}$$

Here, K is a constant which can be evaluated by calibration of the PLL. Eq. (6) shows that the PLL output $i_P(t)$ is proportional to the instantaneous surface velocity. This FM demodulation technique is effective to obtain the amplitude A and phase ψ, and to detect transient signals as well as continuous vibration signals. The detail description of the PLL can be found in Ref. (10)

3. Construction of the LDV System

3.1 Optical System

The optical arrangement for the LDV system for in-plane vibration measurements is shown in Fig. 2. All optical components are mounted on a stable optical bench and a probe head is mechanically decoupled from the bench using optical fibers. A coherent beam from a polarized 10mW He-Ne laser is divided into two beams. For heterodyne detection[8], one of the two beams is frequency-shifted by an acousto-optic Bragg cell driven at a frequency of 40 MHz. Both beams are coupled into polarization maintaining single mode fibers with microscope objectives, and carried to a laser probe head.

The probe head has been designed to take full advantage of optical fiber technology. This allows the probe head to be compact, and to be scanned along the structure. The probe head consists of two

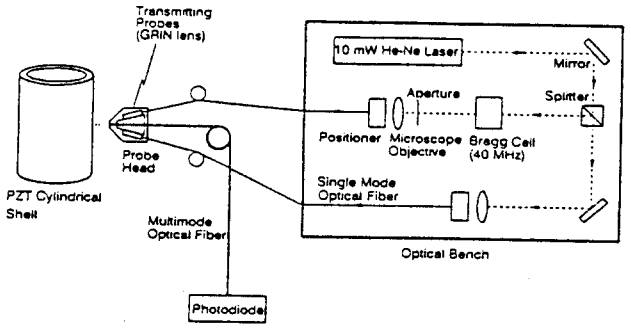

Fig 2 Optical arrangement.

graded-index (GRIN) cylindrical rod lenses as the transmitting optics. Each of two GRIN lenses are mounted on a single plastic (Lexan) platform (3 cm×3cm×0.7cm) so that the angle between the two incident beams is 22°. Each of two optical fibers is carefully positioned relative to each GRIN lens (with a small gap between the fiber and the lens) so that the lens focuses the incident light on the vibrating surface at a distance of 1.5cm, and the same polarization state is kept for the two incident beams. The leveling screw (mounted on the platform) underneath each lens is then adjusted so that the two projecting beams are in the same plan and focused on the same spot on the vibrating surface. As the receiving optics, a multi-mode fiber (3M, FT 1.0-UMT, core diameter 1000μm) is used to directly collect the scattered light from the surface of the structure. Thus, the end of the multi-mode fiber forms a pick-up probe without any collecting lens. The multi-mode fiber is placed at the bisector of the two projecting beams. The multi-mode fiber also transfers the scattered light to an avalanche photodiode (RCA C30950EL).

Typical operating conditions for the LDV system are as follows. There are significant losses in light power when the light is coupled into a single mode fiber. The light power in each of the beams incident on the vibrating surface is 1.7 mW. Each of the beams is focussed on the surface to a circular spot with a size of about 50μm. Light is reflected diffusively in all directions by the metallic rough surface (which is rough on the scale of an optical wavelength). The average light power received by the photodiode is about 2.5μW

3.2 Detection System

A schematic diagram for the detection system is shown in Fig. 3. The output signal (40 MHz FM signal) from the photodiode is adequately amplified and mixed with a 40.1 MHz signal generated by a crystal oscillator. Mixing the signals produces a carrier signal down-shifted to a frequency of 100 kHz. After the 100 kHz FM signal is amplified and filtered, it is sent to the PLL. The output signal from the PLL is the vibration signal proportional to the instantaneous surface velocity as shown in Eq. (6) The vibration signal is displayed on a digital oscilloscope. In order to transfer the vibration signal data from the oscilloscope to a system computer, a GPIB (general purpose interface bus) board is used.

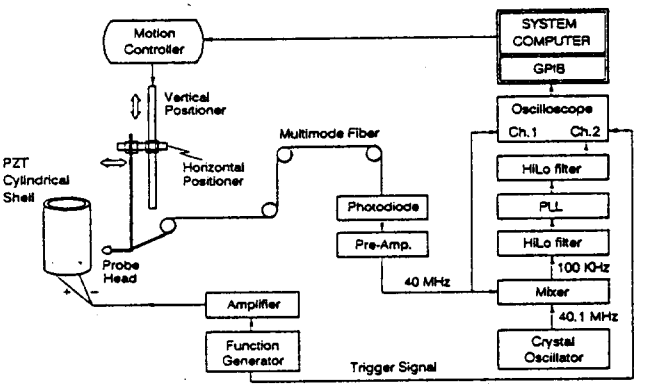

Fig 3 Schematic diagram for the detection and scanning system.

3.3 Self-Alignment Algorithm

In order to obtain a reliable vibration signal, the two laser beams should be focused on the same spot on the vibrating surface. The alignment of the probe head is very sensitive to the surface conditions such as surface roughness and positional errors of an experimental model. Realignment of the probe head should be performed at each data points on the vibrating surface to obtain a reliable vibration signal. In order to achieve the automated alignment of the probe at each data point, the following self-alignment algorithm has been developed.

Figure 4 shows a typical pattern of rms value of the 40 MHz FM signal as a function of the horizontal distance of the probe from the vibrating surface. A reliable vibration signal can be acquired at the position of the probe at which the rms value of the 40 MHz FM signal is a maximum. At an initial data point on the vibrating surface, alignment is manually performed to find the optimum point with the maximum rms value of the 40 MHz FM signal. This optimum point is used as an assumed optimum point when the probe head is repositioned to the next consecutive data point. Once the probe head is re-

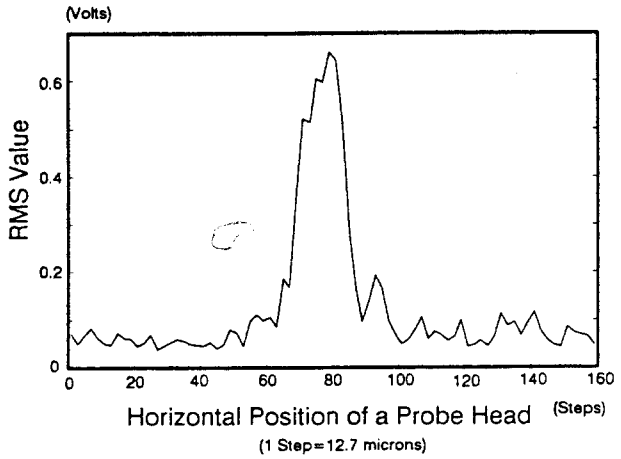

Fig 4 Typical pattern of rms values of a 40 MHz FM signal from the photodetector.

positioned to the next data point, a horizontal distance (e. g. $\pm 800\mu$m) around the assumed optimum point is scanned. Every 25μm, a rms value of the 40 MHz FM signal is directly acquired from Channel 1 on the oscilloscope. Comparing the rms values, the location of the new optimum point is detected. Once the probe head moves back to the optimum point, the vibration signal is averaged to improve the signal to noise ratio at the oscilloscope. The averaged vibration signal is acquired from Channel 2 on the oscilloscope, and stored as a data file in the system computer. The same procedure is repeated at the next consecutive data point. All those procedures are controlled by a computer program except for the manual alignment at the initial data point.

3.4 Scanning Control and Measurements

The measurements are automatically performed by scanning the probe along the surface of an experimental model, and by focusing the two laser beams on the same spot at each data point. Figure 3 shows the schematic diagram for the scanning system. Scanning is accomplished by means of a motor-driven vertical positioner. (A horizontal positioner and a rotary table can be assembled to make 2-D rectangular scan and 2-D cylindrical scan, respectively.) The probe head is fixed at the end of the aluminum rod. The rod is mounted on a horizontal positioner, which provides horizontal movement to focus the two beams on the surface of an experimental model. The horizontal positioner has enough fine resolution (12.7μm advance per step with accuracy within 0.0125cm/m) to achieve focussing of the two beams. The system computer controls scanning of the probe, monitoring of signals, focussing of the two laser beams on the vibrating surface and data acquisition by means of the self-alignment algorithm.

4. Performance Tests of the System

The first experiment was performed with a continuous single frequency signal. The experimental model was a PZT (piezoelectric) cylindrical shell of length $l=3.8$cm, mean radius $r_m=1.737$cm and thickness $t=0.328$cm. The shell has the material property such as piezoelectric constants $d_{13}=135\times 10^{-12}$m/V, $d_{23}=135\times 10^{-12}$m/V and $d_{33}=300\times 10^{-12}$m/V where 1, 2 and 3 denote the axial, circumferential and radial directions, respectively. The reason for use of the PZT shell is that one can precisely evaluate the displacement field over the shell vibrating in air at low frequencies where inertia effects can be neglected[11]. The shell was vertically put on three pieces of corprene. It was continuously driven at 1 kHz and 3 kHz, respectively, by 39 volts. Measurements were automatically performed by scanning the laser probe along the shell.

The second experiment was performed with a pulse signal. The experimental model was an aluminum plate of width $W=183$cm, height $L=122$cm and thickness $h=1.25$cm as shown in Fig. 5. The plate was held vertically between two supporting frames of a platform with four pieces of neoprene located uniformly along upper and lower sections, respectively. The plate was excited by four piezoelectric shakers (made in the U. S. Naval Research Lab.) driven with a pulse which is a 2-cycle pulse (cosine function) of 8.5 kHz. Each two shakers are mounted at the upper section along a length of 13 cm symmetrically relative to the center-line of the plate. The length of 13 cm corresponds to about 0.2 times wavelength of an in-plane wave (longitudinal wave) propagating over the plate at 8.5 kHz. Scanning was performed along a length of $0.7L$, which is located below the upper section along a center-line of the

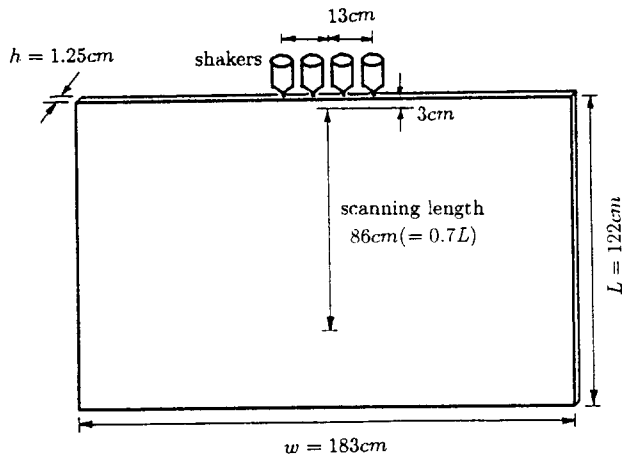

Fig 5 Experimental model (aluminum plate) driven by 4 shakers.

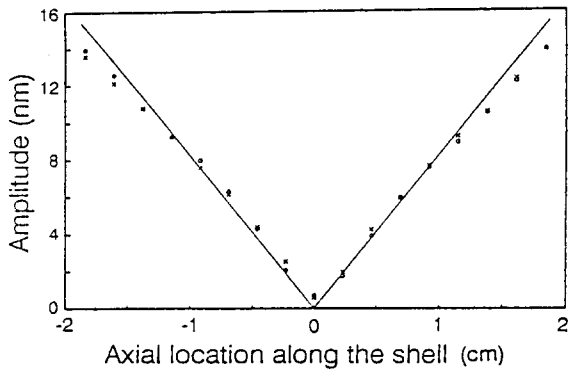

Fig 6 Axial displacements along the PZT shell driven at 1 kHz (ooo) and 3 kHz (x x x), respectively. The solid line corresponds to the theoretical prediction.

plate. The self-alignment computer program was applied to detection of the vertical components (in -plane components) of displacements at 64 points over the plate.

5. Results and Discussions

The automated scanning LDV system was tested on the PZT cylindrical shell as described at the previous section. The shell was driven with continuous signals of 1 kHz and 3 kHz, respectively. The axial displacements at 16 points along the PZT cylindrical shell were measured. Figure 6 shows the experimental results for the in-plane axial displacement field along the shell driven at 1 kHz and 3 kHz, respectively. The experimental results show good agreement with theoretical predictions within 1nm accuracy. (The theoretical displacement field over the shell can be evaluated with the known piezoelctric contstants and the input voltage applied between the outer and inner surfaces[11].)

The automated scanning LDV system was also tested on the plate, as described at the previous section. The plate was driven with a 2-cycle pulse with a center frequency 8.5 kHz. The in-plane displacement field along the center-line of the plate was measured. The displacement field can be regarded as superposition of disturbances due to elastic waves propagating over the plate[12]. The experimental data is decomposed into contributions of the elastic waves as follows. Consider the vertical (in -plane) component $v(0, y, t)$ of the displacement along the center line ($x=0$) over the surface of the plate. The contribution of each wave is expressed as the Fourier transform of $v(x, y, t)$ which takes the form[12]

$$V(k_y, f) = \frac{1}{2\pi}\int_{-\infty}^{\infty}\int_{-\infty}^{\infty} v(0, y, t)\, e^{ik_y y} e^{-i2\pi ft} dydt \tag{7}$$

where f and k_y correspond to the frequency and the wavenumber in the vertical direction, respectively. Here, $V(k_y, f)$ physically represents the complex amplitude of a wave propagating in the direction of the related wavenumber vector whose vertical component corresponds to k_y. The complex amplitudes $V(k_y, f)$ are evaluated by taking the temporal and spatial Fourier transforms into $v(0, y, t)$. Figure 7 shows the wavenumber spectrum which corresponds to the three dimensional plot of magnitudes of the complex amplitudes in the wavenumber-frequency plane. Strong peaks appear in the low wavenumber region between 5 kHz and 14 kHz. Those are associated with longitudinal waves, which have a large in-plane motion along the center line of the plate. Weak peaks are also found in the high wavenumber region. Those correspond to flexural waves. Those might be excited by the bending motion of the plate, which was due to the positional error of the shakers normally mounted at the upper section of the plate. The peaks in the wavenumber spectrum provide the

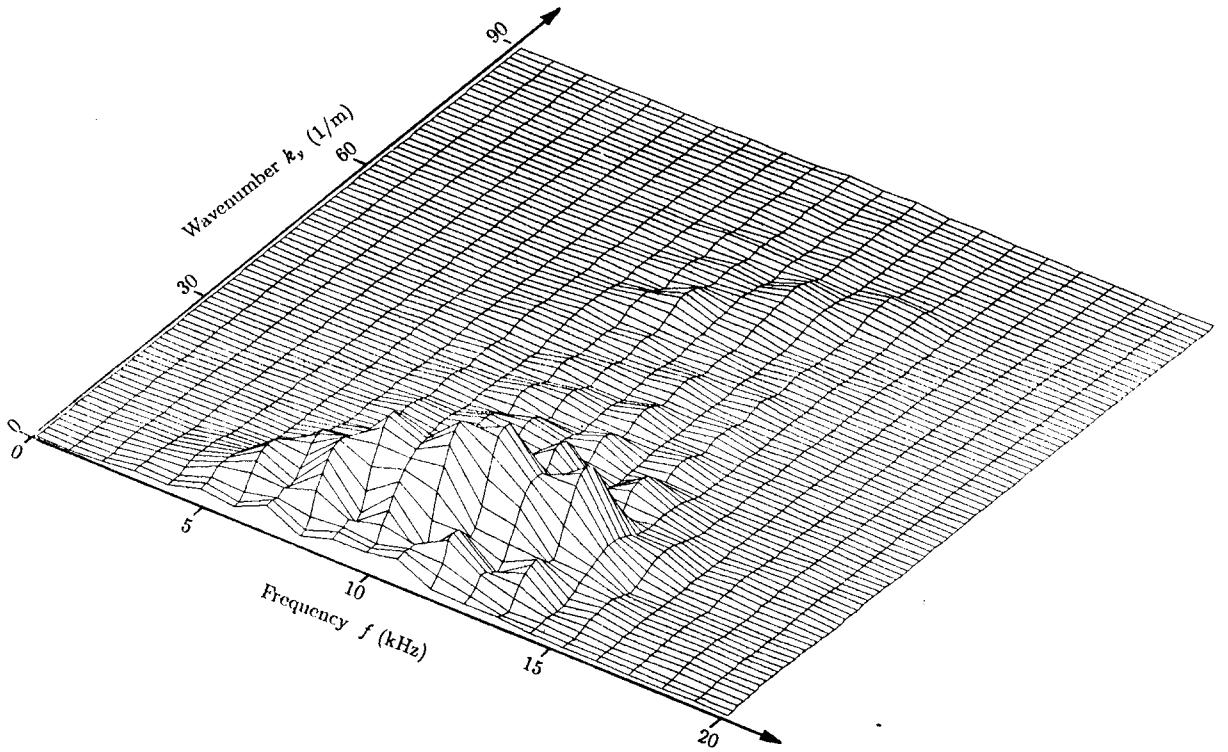

Fig 7 Experimental result for wavenumber spectrum of vibration field along the center-line of the plate.

outline of dispersion curves for waves propagating on the plate. Those are compared with the theoretical dispersion curves, which are calculated from the equations of motion for thin plates[13]. The comparison shows good agreement between two results for flexural and longitudinal waves as shown in Fig. 8.

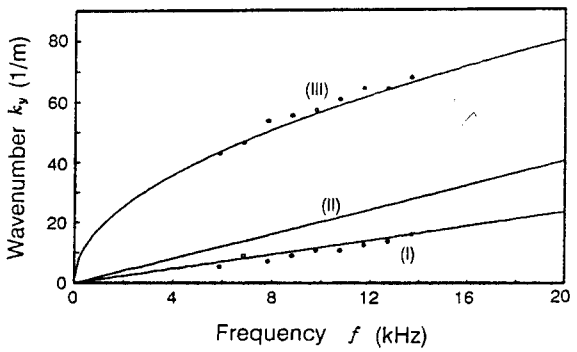

Fig 8 Dispersion relation of waves propagating on the plate. (◦◦◦) denotes experimental results and solid lines correspond to theoretical predictions for (I) longitudinal waves, (II) shear waves and (III) flexural waves.

The performance characteristics of the present system were determined as follows: (1) The minimum detectable displacement amplitude was determined experimentally to be ~1 nm in the frequency range of 500 Hz~20 kHz with a variable bandwidth between 1 kHz and 10 kHz in the receiving electronics, and with 64 times signal averaging to reduce noise. (2) The accuracy of the displacement measurement was determined by comparing the present system with measurements made using a calibrated accelerometer. The LDV measurements agreed with the accelerometer to within~1nm. (3) The repeatability of the measurements was also found to be~1nm. (4) The dynamic range of the system, for the displacement measurements, is 50 dB. The lower limit is the minimum detectable displacement of 1 nm. The upper limit is set by the maximum deviation (~40 kHz) in frequency which the PLL can track. This corresponds to a displacement of ~300nm at 10 kHz. (5) The frequency range of the system is set by the PLL demodulator. The present PLL allows one to measure the signals over the

range 200 Hz~20 kHz. At frequencies below 200 Hz environmental noise (temperature fluctuations and vibration) increases significantly in the system.

The above performance characteristics are not necessarily the best possible values for the LDV system. For example, an analog PLL was used as the FM demodulator because it is inexpensive and readily available. Possibly better demodulation performance may be obtained with digital signal processing.

6. Conclusions

An automated scanning lasder Doppler vibrometer has been designed and built to measure the in-plane vibration of structures. The self-alignment algorithm was introduced, which allowed the system completely automated to get extensive data for vibration field over the structures. The algorithm can be used to detect transient vibration signals as well as continuous vibration signals. Those results show that the automated scanning LDV system can be a useful tool to measure the in-plane vibration and to detect the elastic waves propagating on the vibrating structures.

References

(1) Fahy, F., 1985, Sound and Structural Vibration, Academic Press, Chap. 1.

(2) De Jong, C. A. F. and Verheij, J. W., 1993, "Measuremet of Vibrational Energy Flow in Straight Fluid-Filled Pipes: A Study of the Effect of Fluid-Structure Interaction," Proceding of the 4 th International Congress On Intensity Techniques, Senlis, France, pp. 111~117.

(3) Monchalin, J. -P., Aussel, J. -D., Heon, R., Jen, C. K., Boudreault, A. and Bernier, R. , R., 1989, "Measurement of In-Plane and Out-of-Plane Ultrasonic Displacements by Optical Heterodyne Interferometry," Journal of Nondestructive Evaluation, Vol. 8 (2), pp. 121~133.

(4) Vignola, J. F. and Houston, B. H., 1993, "The Design of a Three Dimensional Laser Vibrometer," ASME Winter Annual Meeting, 93 -WA/NCA-10.

(5) Sriram, P., Hanagud, S., Craig, J. and Komerath, N. M., 1990, "Scanning Laser Doppler Techniaue For velocity Profile Sensing On a Moving Surface," Applied Optics, Vol. 29(6), pp. 2409 ~2417.

(6) Dominguez, J. C. L, and Wicks, A. L., 1995, "Reconstruction of 3-D Structural Velocity Field of a Vibrating Turbine Blade Using a Scanning Laser Doppler Vibrometer," Proceedings of the 13 th International Modal Analysis Conference, Nashville.

(7) Lee, D., Berthelot, Y. H. and Jarzynski, J., 1990, "A Study of Wave Propagation On a Cylindrical Shell Using Fiber Optic Laser Doppler Velocimetry," Journal of Acoustical Society of America, Vol. 94(1), pp. 196~212.

(8) Lading, L., 1970, "Dfferential Doppler Heterodyning Technique," Applied Optics, Vol. 10, pp. 1943~1949.

(9) Hanish, S., 1983, "Underwater Laser Doppler Hydrophone," A Tretise on Acoustic Radiation, Vol. 2, pp. 377~397.

(10) Best, R. E., 1984, Phase-Locked Loops, McGraw-Hill, pp. 1~68.

(11) Wilson, O. B., 1988, Introduction to Theory and Design of Sonar Transducers, Peninsula Publishing, pp. 42~62.

(12) Pierce, A. D. and Kil, H. -G., 1990, "Elastic Wave Propagation From Point Excitations on Thin-Walled Cylindrical Shells," Journal of Vibration and Acoustics, Vol. 112, pp. 399~406.

(13) Junger, M. C. and Feit, D., 1993, Sound, Structures, and Their Interaction, Acoustical Society of America, Chap. 7.